ORIGINAL ARTICLE

Study on distribution characteristics of some water parameters properties of mine drainage in an oxidation pond, Hwangji-Yuchang coal mine, South Korea

Dong-kil Lee · Gil-Jae Yim · Sang-Woo Ji · Young-Wook Cheong

Abstract Tracer test, in situ distribution test, and computational flow analysis at an oxidation pond, consisting of passive treatment system treating coal mine drainage at the Hwangji-Yuchang coal mine in South Korea were performed to identify the distributed physicochemical and rheological characteristics of the acid mine drainage. The influent mine water that flowed into the oxidation pond was at pH 6.79 and had 25.5 mg/l of ferrous iron concentration and the flow rate was 59.3 m^3/h. As a result of the studies, oxidation of Fe^{2+} in the oxidation pond was found to have mostly occurred near the inlet of the pond. The distribution of the physical properties such as pH, dissolved oxygen, electric conductivity, total dissolved solid, turbidity, ferrous concentration, oxide reduction potential and water depth in the oxidizing pond was found to have been directly affected by the ferrous iron oxidation rate and rheological characteristics of the influent.

Keywords Acid mine drainage · Oxidization pond · Physicochemical characteristics · Rheological characteristics

Introduction

Passive treatment systems to purify mine water can be maintained at a lower cost than conventional treatment plants and can be installed at abandoned mines in remote locations (Perry and Kleinmann 1991; Skousen et al. 1998). Two passive treatment systems can be used comprising an

D. Lee (✉) · G.-J. Yim · S.-W. Ji · Y.-W. Cheong
Korea Institute of Geoscience and Mineral Resources (KIGAM),
Daejeon, Republic of Korea
e-mail: ldk@kigam.re.kr

oxidation pond, Successive Alkalinity Producing Systems (SAPS) and wetland, or SAPS, oxidation pond and wetland system depending on water quality. An oxidation pond is designed to hold acid mine drainage (AMD) for a detention time, during which Fe^{2+} is oxidized by dissolved oxygen (DO) before settling as iron hydroxide.

The design of an oxidation pond is usually based on either an empirical iron removal rate derived from the performance of aerobic wetlands (Hedin et al. 1994) or by defining a nominal retention time. Engineering design guidelines for oxidation ponds were suggested by the National Coal Board (NCB) (Banks 2003). The NCB (1982) recommended the capacity of an oxidation pond to be 1 l/sec per 100 m^2 of the pond area and nominal retention time was defined as 48 h (Laine and Jarvis 2003). The depth of the pond was constructed to be 3 m, in general, that was considered to be the necessary depth to prevent the settled particles from refloating by wind or horizontal flow (PRAMID Consortium 2003). Additional guidance on retention time of mine water can be drawn from studies conducted in the United States (Keefe et al. 2004; Lin et al. 2003) and in UK reducing and alkalinity producing systems (Wolkersdorfer et al. 2005), and modeling studies (Goebes and Younger 2004). Recently, Kruse et al. (2009) carried out measuring the retention time of mine water in oxidation ponds and wetlands using Bromide.

Using guidelines that are based on observations explains the difficulty to accurately formulize the effect of the lumped processes of ferrous oxidation, oxygen transfer, and settling velocities encountered for mine waters of different pH and chemistry (Sapsford et al. 2007). When the mine water flows into the oxidation pond from a mine or SAPS, the reducing environment for the mine water is changed to an oxidizing environment and the amount of dissolved oxygen is increased. Ferrous iron contained in

the mine water could be converted to Fe^{3+} through an oxidation reaction severely depending on pH and DO, which is then precipitated in the form of $Fe(OH)_3$. The $Fe(OH)_3$ formation process is pH dependent and occurs rapidly when pH > 4 (Stumm and Morgan 1996). When AMD is neutralized, its dissolved metals precipitate as low density flocculates (floc or sludge) of metal hydroxyl sulfates (Nordstrom 1982; Sterner et al. 1998; Thomas and Romanek 2002). During such a process, the mine drainage undergoes various physicochemical variations, which likely represent various distribution characteristics in the oxidation pond.

Most of the studies on oxidation ponds focus on the retention time of mine water for each pond design. However, no investigation has ever assessed the actual distribution of physical–chemical properties of mine drainage in an oxidation pond. Thus this study was intended to carry out a tracer test using Blue #2 dye, an in situ distribution test and computational flow analysis for an oxidation pond where influent mine water with a neutral pH has been flowing. In addition, a comprehensive analysis of distribution of physical–chemical parameters within the oxidation pond [pH, DO, electric conductivity (EC), total dissolved solid (TDS), turbidity, ferrous concentration, oxide reduction potential (ORP) and water depth] was completed, to delineate the redox processes occurring in different zones of the oxidation pond.

Site determination for tests

The Hwangji-Yuchang oxidation pond in Gangwon Province, South Korea was selected as the study site. The pond was 46 m × 38.7 m with a 1 m depth. The mine water from the portal is drained through a gently sloping 100 m long pipe leading to the oxidation pond. The dissolved oxygen concentration, measured in influent, at the end of the pipe was 7.9 mg/l as a result of aeration due to turbulent flow through the watercourse. The influent had the pH of 6.79, which was close to neutral. The influent water is introduced by gravity above the water surface in the oxidation pond through a pipe (0.5 m ID), and flows out through an outlet located 20 cm below the water surface (Fig. 1).

Experimental method

In situ distribution test (measurement of water quality parameters)

Figure 2 shows the diagram of the Hwangji-Yuchang oxidation pond. As indicated in Fig. 2, the surface of oxidation was divided into a regular spaced grid where each of

Fig. 1 Hwangji-Yuchang oxidation pond

sections was 7 m long both in the vertical and horizontal directions. There were a total of 30 measuring point stations, including the inlet and the outlet. Water samples were taken at 10–20 cm below the water surface to minimize the contact with the air using a small boat at all measuring points.

The water parameters measured were pH, DO, EC, TDS, Turbidity, Ferrous iron concentration, ORP, and water depth at each station. The pH and DO were measured using pH meter (TOA's HM-20P); EC and TDS were measured with Conductivity Meter (ORION's 125A+); turbidity was measured by Turbidimeter (HACH's 2100P); and the ferrous iron concentrations were determined with the 1,10 phenanthroline method (HACH's DR/2800 colorimeter; HACH 2009).

The depth of the study pond was 1 m and the water level of AMD is maintained at approximately 0.8 m. However, the effective water depth is less than 0.8 m because of sedimentation of the iron hydroxide. When measuring the depth from the surface to the sediments, a low specific gravity device with a large contact area was constructed to prevent disturbing the iron hydroxide at the bottom.

Tracer test

The tracer test was conducted to identify the distribution pattern and retention time of the mine water which flowed into the pond. The edible Blue #2 dye used has a low environmental impact and its flow route was easily traced by visual observation. The flow rate of the influent mine drainage was measured using a pre-installed flowmeter, as shown in Fig. 3a. Variation of the flow rate of the influent is indicated in Fig. 3b. Mine water with 168 ppm of dye concentration was injected into the pond for 4 min.

Fig. 2 Measuring points at the Hwangji-Yuchang oxidation pond
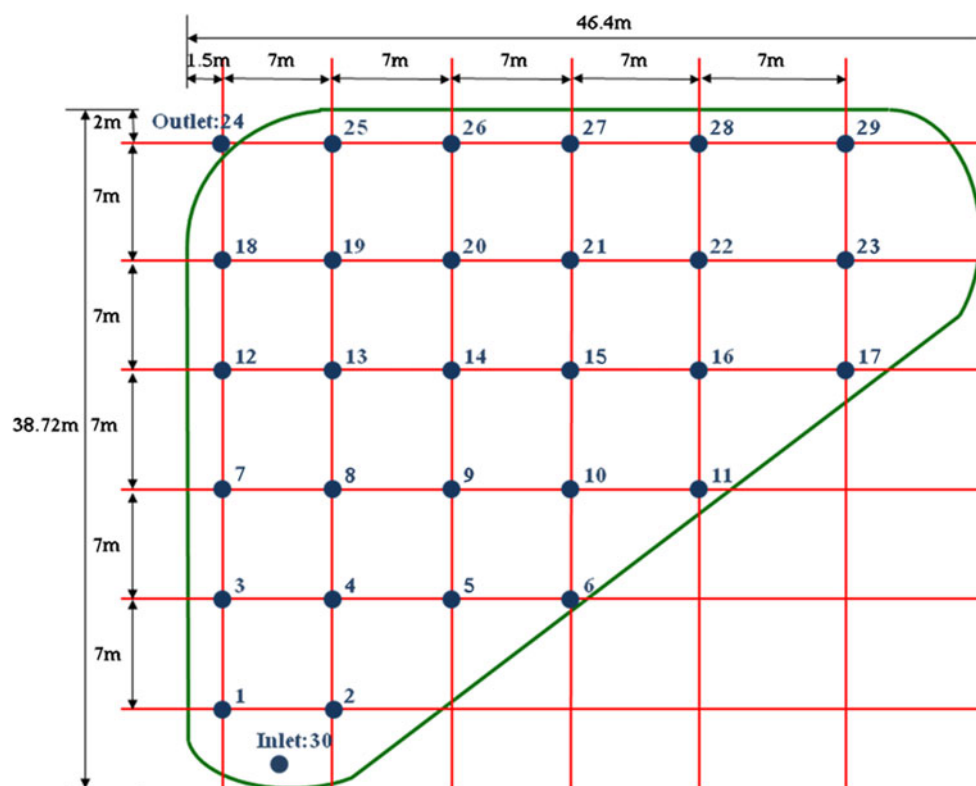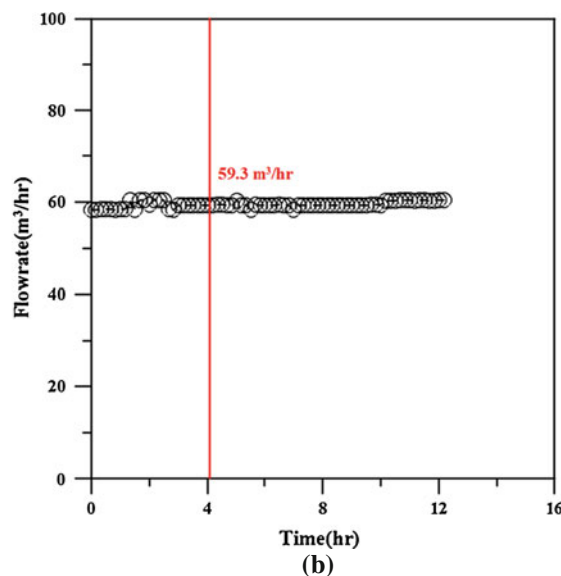
Fig. 3 Flowmeter and variation of flow rate of the mine water in the Hwangji-Yuchang oxidation pond. **a** Flowmeter at the pond, **b** Flow rate of the AMD during test

The flow rate of the water was 59.3 m³/h, which changed minimally over 3 h. An inflow age was determined when the moving dye reached particular points on the grid measurement. The inflow age of the tracer dye was recorded at each of the 30 stations, to determine the flow pattern and retention time of the influent for the pond.

Computational flow analysis

The flow analysis was conducted using FLUENT (ANSYS 2012), a computational fluid dynamics program, to identify the flow characteristics and used to calculate the retention time of the mine water in the oxidation pond. The air age

concept, used in air conditioning systems, was applied to calculate the inflow age, which is defined as the time taken for the influent to move to a certain point in an oxidation pond. The continuity equation, momentum equation, and k-ε turbulent equation were designated as governing equations and the analysis was conducted under the steady state condition. Given that mine water that flowed into the oxidation pond was constantly maintained at 59.3 m³/h, the constant flow rate and pressure conditions were assigned as boundary conditions for the inlet and the outlet, respectively. To identify the distribution of the inflow age of the mine water, this variable was calculated with a user defined scalar.

Figure 4 shows the grids designed for flow analysis of the Hwangji-Yuchang oxidation pond. The meshes were denser near the inlet, outlet, water surface and wall and the grid sizes were increased gradually as the model

approached the middle of the pond. The total number of grids in the pond was up to 1 million and maximum skewness is under 0.3.

Results and discussion

Flow characteristics of the mine water in the oxidation pond obtained by computational flow analysis

Figure 5 shows the result of the computational flow analysis of the oxidation pond. Based on the velocity distribution on the surface of the oxidation pond in Fig. 5a, high velocity appeared along the side between the inlet and the outlet while the velocity on the right side of the pond was very low. As the flow line distribution indicated in Fig. 5b, the governing flow of the mine water starts from the inlet
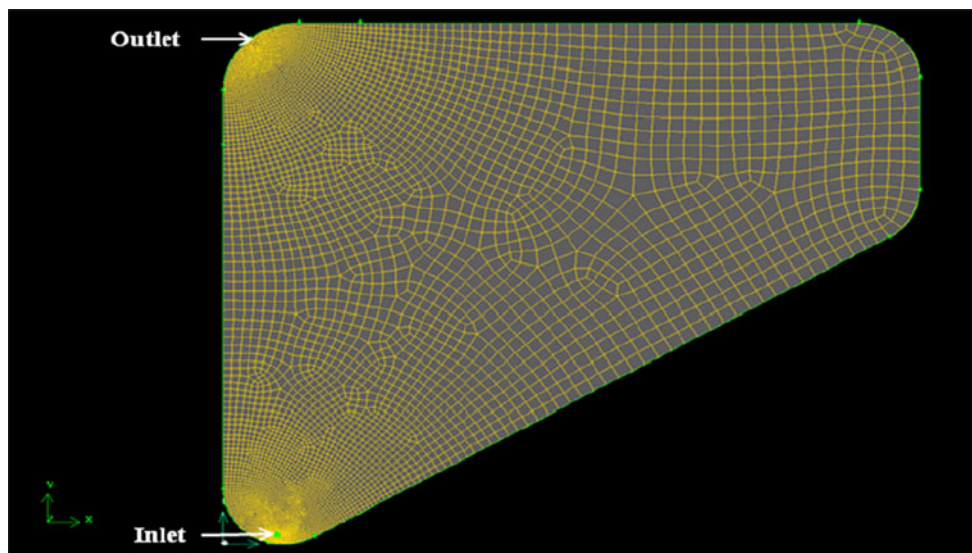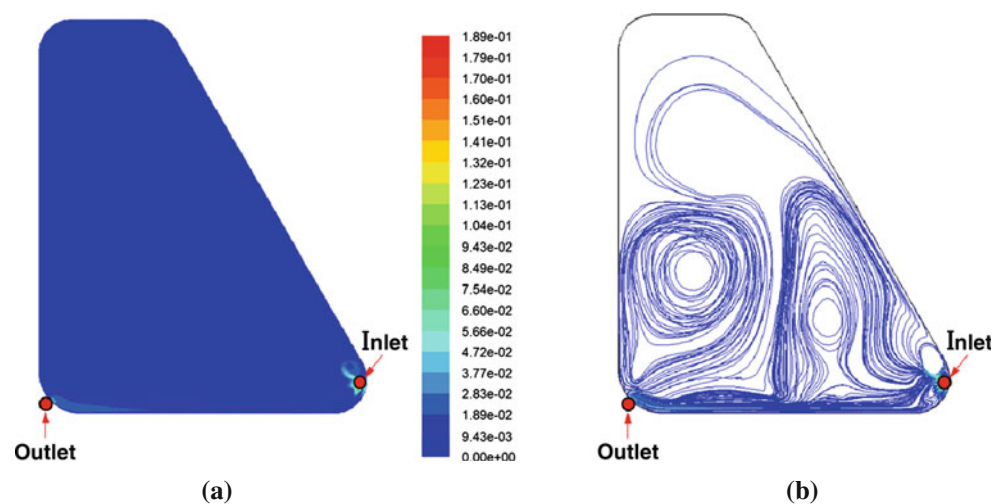

Fig. 4 Grids of the Hwangji-Yuchang oxidation pond for computational flow analysis

Fig. 5 Flow distribution using the computational flow analysis in the Hwangji-Yuchang oxidation pond. **a** velocity distribution, **b** flow line distribution

and goes to the outlet along the left wall. The flow on right side indicates a lengthy territory that extended to the outlet, forming two large eddies. So the mine water in the Hwangji-Yuchang oxidation pond flowed to a specific area, not over the entire area of the pond. The flow area was categorized into a main flow area and a stagnant area.
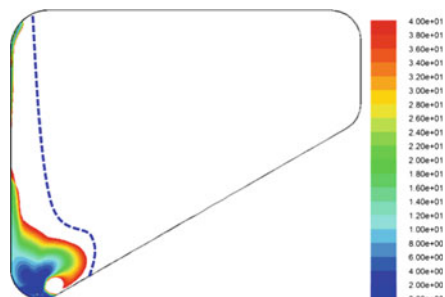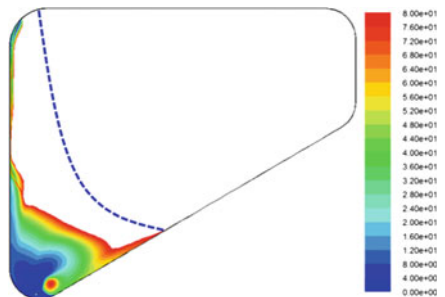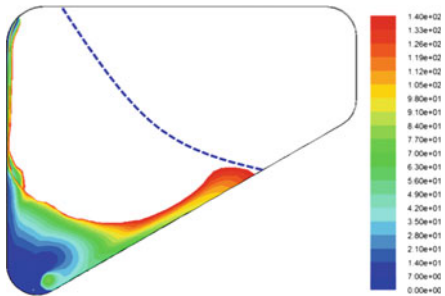
Water parameter measurements and tracer test

Contouring of water parameters represented by Kriging method.

1. Inflow age and retention time

Retention time of the mine water was obtained using dyes in the oxidation pond and the flow distribution and travel time of the dyes are indicated in Table 1. The mine water reached the outlet of the oxidation pond in 40 min. The dyes moved from the inlet to the outlet along the left wall as shown in Table 1, which was the same result as the computational analysis. The dye began spreading toward the right of the pond after 40 min. The dye had yet to expand to the entire area of the pond 2 h 40 min after injection. The blue line in Table 1 is the line estimating the spread of the dye. As seen in Table 1, the dye spread range and inflow age in the computational analysis corresponded relatively well with each other. Based on observing the

Table 1 Tracer spread over time in the Hwangji-Yuchang pond

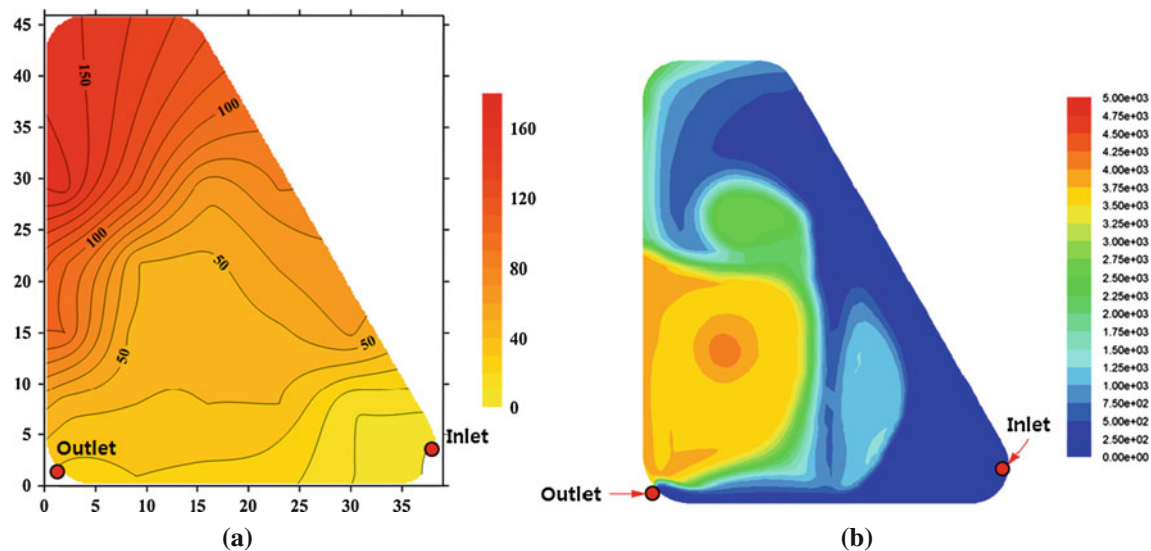| Computational flow analysis	Tracer test
40 min	40 min
80 min	80 min
140 min	140 min

Fig. 6 Distribution of inflow age of the AMD in the Hwangji-Yuchang pond. **a** Inflow age (min) by the tracer test, **b** Inflow age (min) by the computational flow analysis

behavior of the dye dispersion over time, the mine water mostly moved along the shortest path between the inlet and the outlet, and a very little flow was monitored in other areas.

The results of the inflow age distribution by the tracer test and the computational analysis are presented in Fig. 6. During the first 40 min after adding the dye, the dye diffused toward the right at the outlet as shown in Fig. 6a. A contour became dense after 50 min of inflow age, which resulted from stagnant flow of the mine water and the dyes moved by diffusion alone in this area. Thus, the territory was divided into a main flow area and a stagnant area when the inflow age reached 40–50 min. Such a result appeared in the computational analysis in Fig. 6b. Viewing the distribution of the inflow age, it was shorter at the sides between the inlet and outlet, while it extended in the stagnant area on the right.

2. Ferrous iron concentration

The ferrous iron concentration of the mine water in the pond is illustrated in Fig. 7a. The highest concentration was found at the area nearby the inlet and it significantly decrease as the distance from the inlet increase. The pH of the mine water in the pond was 6.79 on average, which was close to the neutral 7, meaning that mine water with neutral pH could be a favorable condition for the oxidation of ferrous iron to ferric iron near the inlet. In contrast to the higher ferrous iron concentration at the inlet, the ferrous iron concentration over the entire area of the pond appeared to be around 10 mg/l.

3. Electric conductivity

Figure 7b shows the distribution of EC in the Hwangji-Yuchang oxidation pond. The EC was rapidly reduced near the inlet and was gradually reduced toward the outlet along the main flow. In contrast, the EC appeared to be constant in the stagnant area of the pond. Since the EC is related to the total dissolved ions in the water, it appeared to be higher at the inlet where the ferrous iron concentration was high, and further from the inlet, the ferrous ion concentration of the mine water decreased due to the ferrous oxidation reaction, so the EC tended to decline further from the inlet. In the stagnant area, the EC seemed to become constant.

TDS refers to the total solids which are dissolved in the water such as organic material, inorganic material, ions, and salts. Salinity is related to the salts contained in the water and thus it is closely related to the EC. So the distribution tendencies of TDS and salinity are similar to that of the EC. The mine water that flowed into the pond had a high ferrous iron concentration, and a high TDS and salinity, and, in line with the process of precipitation in the pond, the ferrous iron concentration decreased along with the TDS and salinity.

4. Dissolved oxygen

Figure 7c shows the distribution of DO in the oxidation pond. It shows the high DO near the inlet which was rapidly reduced as the mine water moved outward, which was attributable to active iron precipitation near the inlet. The DO gradually was reduced along the main flow from the inlet to the outlet of the pond. Distribution of DO in the
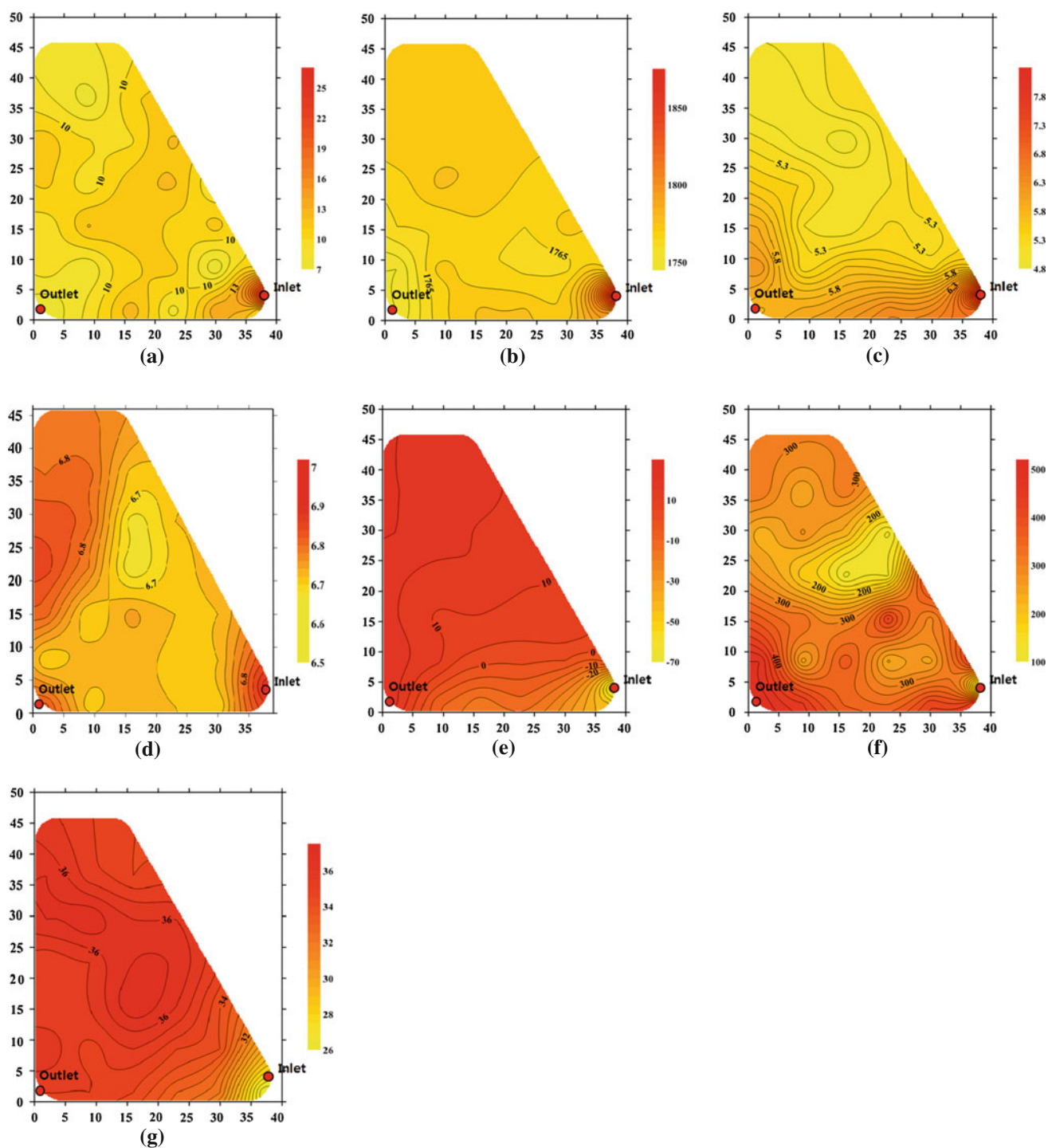
Fig. 7 Distribution of physical–chemical parameters within the oxidation pond. **a** Ferrous iron concentration (mg/l), **b** Electric conductivity (μS/cm), **c** Dissolved oxygen (mg/l), **d** pH, **e** Oxide Reduction Potential (mV), **f** Turbidity (NTU), **g** Water depth (cm)

pond seemed to reflect the flow characteristics of the mine water.

5. pH

Figure 7d shows the distribution of pH in the pond. The pH was higher at the inlet and reduced when moving outward. When the ferrous iron in the mine water is hydrolyzed to form hydroxide, it produces free hydrogen (H^+) causing the pH of mine water to lower. On the other hand, the pH increased a little in the stagnant area and this was attributable to variation of the components of the mine water.

Table 2 Variation of the water parameters at the inlet and outlet in the oxidation pond

Properties	Inlet	Outlet	Removal efficiencies (%)
Fe^{2+} (mg/l)	25.5	7.1	72.2
DO (mg/l)	8.12	5.78	28.8
pH (−)	6.79	6.7	1.3
EC (μS/cm)	1,872	1,750	6.5
TDS (mg/l)	942	878	6.8
ORP (mV)	−66.2	16.4	−124.8
Temperature (°C)	16.0	19.6	−22.5
Turbidity (NTU)	134	496	−270.1

6. ORP

As the mine water spread over the oxidation pond, the ORP changed to a reduction condition (Fig. 7e). The ORP rapidly increased as the mine water moved away from the inlet. Notably, based on observing the gradient of the ORP along the main flow in Fig. 7e, the ORP represented the relationship between the flow characteristics and iron oxidation reaction in the pond. In the stagnant area, the mine water exhibited a high and constant ORP.

7. Turbidity

Figure 7f represents the distribution of turbidity in the Hwangji-Yuchang oxidation pond. In the mine water that flowed into the pond, active iron precipitation occurred and thus a relatively higher turbidity was indicated near the inlet. But the image showed significant turbidity variation also in the stagnant area, which was caused by refloating deposits due to convection flow of the mine water resulting from temperature differences.

8. Water depth of the oxidation pond

Figure 7g shows the distribution of water depths of the Hwangji-Yuchang oxidation pond. Iron precipitation from the mine water occurred rapidly near the inlet and thus the deposits intensively accumulated near the inlet. The depth tends to be the lowest near the inlet and increases gradually along the main flow. In contrast, the depth in the stagnant area was maintained at 36 cm with little variation.

Variation of the mine water parameters that flowed into or out of the pond is shown in Table 2. Considering the near neutral pH, the distribution of the mine water parameters in the Hwangji-Yuchang oxidation pond was found to have been directly affected by the iron precipitation reaction rate and flow characteristics of the AMD. The removal efficiency of Fe^{2+} in the pond was as much as 72.2 %. The mine water with 8.12 mg/l of DO aerated before flowing into the pond decreased to 5.78 mg/l by ferrous oxidation. Ferrous oxidation and $Fe(OH)_3$

formation process made 0.09 of pH dropped and EC and TDS to the similar decreasing percent of 6.5 and 6.8, respectively. ORP was increased from −66.2 mV to 16.4 mV because the reducing environment for the mine water is changed to an oxidizing environment when the mine water flows into the oxidation pond. The discharge of the water was higher temperature of 3.6 °C than the influent on account of daytime temperature and the turbidity of the discharge was shown 2.7 times compared with the influent owing to iron precipitation formation.

Conclusion

The mine water introduced into the Hwangji-Yuchang oxidation pond could be divided into a main flow area, linking the inlet to the outlet, and a stagnant flow area. According to the tracer test, the flow distribution was similar to the result of the computational flow analysis. The Fe^{2+} oxidation reaction in the pond mainly occurred near the inlet and thus high gradients appeared on the contouring map for mine water parameters. The ferrous iron concentration, DO, EC, TDS, salinity, and pH rapidly decreased near the inlet and gradually decreases as it flowed closer to the outlet along the main flow, while the ORP, turbidity, and depth increased. The distribution of the DO and ORP are well represented particularly to the inflow age. Hence, the distribution of the water parameters in the oxidation pond has been directly affected by the iron precipitation reaction rate and flow characteristics of the AMD.

References

ANSYS (2012) http://www.ansys.com/Products/Simulation+Techno logy/Fluid+Dynamics/ANSYS+Fluent. Accessed 17 January 2012

Banks SB (2003) The UK Coal Authority Minewater-Treatment Scheme Programme: performance of operational systems. J Chart Inst Water Environ Manag 17(2):117–122

Goebes M, Younger PL (2004) A simple analytical model for interpretation of tracer tests in two-domain subsurface flow systems. Mine Water Environ 23:138–143

HACH (2009) DR 2800 User Manual. HACH Co

Hedin RS, Nairn RW, Kleinmann RLP (1994) Passive treatment of polluted coal mine drainage. USBM IC 9389. US Dept of Interior, Washington DC, p 35

Keefe SH, Barber LB, Runkel RL, Ryan JN, McKnight DM, Wass RD (2004) Conservative and reactive solute transport in constructed wetlands. Water Resour Res 40:1–12

Kruse AS, Gozzard E, Jarvis AP (2009) Determination of hydraulic residence times in several UK mine water treatment systems and

their relationship to iron removal. Mine Water Environ 28:115–123

Laine DM, Jarvis AP (2003) Engineering design aspects of passive in situ remediation of mining effluents. Land Contam Reclam 11(2):113–125

Lin A, Debroux J, Cunningham J, Reinhard M (2003) Comparison of Rhodamine WT and bromide in the determination of hydraulic characteristics of constructed wetlands. Ecol Eng 20:75–88

NCB (1982) Technical management of water in the coal mining industry. National Coal Board, London, p 129

Nordstrom D (1982) Aqueous pyrite oxidation and the consequent formation of secondary iron minerals: acid sulfate weathering. Soil Sci Soc Am Spec Publ 10:37-62

Perry A, Kleinmann RLP (1991) The use of constructed wetlands in the treatment of acid mine drainage. Nat Resour forum 15:178–184

PRAMID Consortium (2003) Engineering guidelines for the passive remediation of acid and/or metalliferous mine drainage and similar wastewaters. Univ Newcatle Upon Tyne, Newcastle, p 166

Sapsford D, Barnes A, Dey M, Williams K, Jarvis A, Younger P (2007) Low footprint passive mine water treatment: field demonstration and application. Mine Water Environ 26:243–250

Skousen J, Rose A, Geidel G, Foreman J, Evans R, Hellier W (1998) Handbook of technologies for avoidance and remediation of acid mine drainage. Natl Mine Land Reclam Cent, Morgantown

Sterner P, Skousen J, Donovan J (1998) Geochemistry of laboratory anoxic limestone drains. In: Proc 15th ASMR Conference, pp 214–234

Stumm W, Morgan JJ (1996) Aquatic chemistry: an introduction emphasizing chemical equilibria in natural waters. Wiley, New York

Thomas R, Romanek C (2002) Acid rock drainage in a vertical flow wetland I: acidity neutralization and alkalinity generation. In: Proceedings of the 19th ASMR Conference, pp 469–585

Wolkersdorfer C, Hasche A, Gobel A, Younger PL (2005) Tracer test in the Bowden close passive treatment system. Wiss Mitt 28:87–92